Eur. Phys. J. B **14**, 495–508 (2000)

THE EUROPEAN PHYSICAL JOURNAL B

EDP Sciences
© Società Italiana di Fisica
Springer-Verlag 2000

Magnetic excitations in charge ordered $\alpha'-NaV_2O_5$

P. Thalmeier[1,a] and A.N. Yaresko[2]

[1] Max-Planck-Institute for Chemical Physics of Solids, 01187 Dresden, Germany
[2] Max-Planck-Institute for the Physics of Complex Systems, 01187 Dresden, Germany

Received 30 April 1999 and Received in final form 5 October 1999

Abstract. An investigation of the spin excitation spectrum of charge ordered (CO) $\alpha'-NaV_2O_5$ is presented. We discuss several different exchange models which may be relevant for this compound, namely in-line and zig-zag chain models with weak as well as strong inter-chain coupling and also a ladder model and a CO/MV (mixed valent) model. We put special emphasis on the importance of large additional exchange across the diagonals of V-ladders and the presence of exchange anisotropies on the excitation spectrum. It is shown that the observed splitting of transverse dispersion branches may both be interpreted as anisotropy effect as well as acoustic-optic mode splitting in the weakly coupled chain models. In addition we calculate the field dependence of excitation modes in these models. Furthermore we show that for strong inter-chain coupling, as suggested by recent LDA + U results, an additional high energy optical excitation appears and the spin gap is determined by anisotropies. The most promising CO/MV model predicts a spin wave dispersion perpendicular to the chains which agrees very well with recent results obtained by inelastic neutron scattering.

PACS. 75.10.Jm Quantized spin models

1 Introduction

Transition metal-oxygen pyramids are ideal building blocks to obtain insulators with low D structures of $3d$-ions like chains or ladders. Their localized spins exhibit collective quantum properties at low temperatures, *e.g.* spin gap formation in $S = 1$ chains or $S = 1/2$ ladders. In addition there is the possibility of spin gap appearance due to the spin-Peierls (SP) mechanism which causes dimerization of the chain. The standard example is $CuGeO_3$ [1]. Recently $\alpha'-NaV_2O_5$ which has the Trellis lattice structure with alternating shifted ladders (Figs. 1 and 6) was investigated for similar reasons: observation of a superstructure below $T_c = 33$ K and subsequent spin gap formation as witnessed by a drop of the susceptibility below T_c [2]. However it is clear now that this compound does not exhibit a standard SP-transition because above T_c it is a homogeneous mixed valent (MV) insulator with one $3d$-electron per V-V rung. Therefore above T_c $\alpha'-NaV_2O_5$ is a quarter filled ladder system with equivalent V-sites instead of a family of half filled (atomic spin) chains. This was concluded from X-ray [3–5] and NMR-experiments [12]. They also show that below T_c in the dimerized state two inequivalent V-sites exist. Therefore a charge ordering (CO) transition which localizes the V $3d$-electrons on one site of each rung of the ladders must take place at T_c. Possible CO-structures have been discussed by various authors [4,8,10] but so far the real low temperature structure remains controversial. In general a CO transition may occur when the *inter*-site Coulomb repulsion is larger than kinetic energy terms, this is only possible in low carrier density semimetals or insulators like $\alpha'-NaV_2O_5$. Charge ordering can be viewed as a Wigner-crystallization on a lattice [6]. This should not be confused with the CDW transition in more metallic systems. The CO-mechanism in insulating $\alpha'-NaV_2O_5$ can be described within an effective frustraded 2D-Ising model[8]. It leads to in-line or zig-zag charge order depending on whether the difference in Coulomb repulsion, K_1-K_2 between n.n. (K_1) and n.n.n. (K_2) is positive or negative respectively. Later we will also discuss alternative CO structures. In reference [8] the possible origin of spin gap formation was discussed for the in-line structure where an induced SP transition slightly below the primary in-line CO transition was proposed. This scenario would naturally explain the appearance of two superposed phase transitions from thermal expansion measurements [9] and the observed anomalous BCS-ratio. As mentioned the zig-zag CO is an alternative possibility, it has been discussed in reference [10] and a related structure in reference [4]. It has been claimed, though not discussed in any detail that this structure leads directly to a gap in spin-excitations.

Important information on the true low temperature CO structure may be obtained from an investigation of the complete dispersion of magnetic excitations, especially along $\mathbf{a}^*$ ($\perp$ to the chain axis $\mathbf{b}$). However the existing neutron scattering results [11] were rather limited in

[a] e-mail: thalm@cpfs.mpg.de

resolution. A special behaviour of excitations for wave vector $\mathbf{q} = (q_x, \pi)$ (in units of $\frac{1}{a}$ and $\frac{1}{b}$) was proposed: the spin gap mode with $\Delta_s = 10$ meV was suggested to be twofold degenerate at $q_x = 0$, 2π and to split into two excitations about 2–3 meV apart for intermediate q_x. This was also discussed in a theoretical model [13]. But more recent experiments with much better resolution [22] have shown that this is definitely not true and a splitting of ~ 1 meV exists even at the points $\mathbf{q} = (0, \pi)$ and $(2\pi, \pi)$. Furthermore new electronic structure calculations [14] based on the LDA + U approach have shown that there is an additional important exchange coupling which has previously been neglected. In addition like in the cuprates small exchange anisotropies may also lead to gaps for spin excitations. Therefore it is desirable to develop a general theory of magnetic excitations in $\alpha'-NaV_2O_5$ that incorporates all these aspects and allows to calculate all possible features of the spin excitations in the various candidate CO-structures of $\alpha'-NaV_2O_5$, including the effect of an external field.

In the following the exchange model for the CO-structures is defined (Sect. 2). For the low temperature CO phases with intra-chain dimerization it may be mapped to a simplified model including only relevant dimer variables (Sect. 3). In Section 4 the spin dynamics of various exchange models for $\alpha'-NaV_2O_5$ will be investigated including exchange anisotropies and external field. The resulting collective magnetic excitations are studied for all models under special emphasis of the importance of intra-chain exchange anisotropies and their influence on the mode dispersions perpendicular to the chain (**b**-) axis. Finally our calculations and their connection to experimental results are summarized in Section 5.

2 Electronic structure, charge order and exchange models

In the high temperature phase ($T > T_c$) $\alpha'-NaV_2O_5$ is an insulating mixed valence compound whose electronic structure is now reasonably well understood [5,14]. In an effective tight binding (TB) model including only V($3d$) orbitals one has bonding (B) and antibonding (AB) bands corresponding to the symmetric and antisymmetric molecular orbitals of each V-V rung. In the following a similar convention for the notation of TB hopping matrix elements is used as for the exchange integrals in Figures 1 and 6. The B-AB gap $\sim \tilde{t}$ is about one eV and the band widths are ~ 0.5 eV (B) and almost zero (AB). This difference has an important origin [14] which was not realized previously: since the dispersion of B and AB bands are proportional to $t + t_d$ and $t - t_d$ respectively it means that $t_d \simeq t$, and hence t_d, the hopping across the ladder diagonal cannot be neglected and is necessary for a realistic TB model of *both* B and AB bands. In a naive superexchange model this would also mean that the AF exchange constants $J \sim \frac{2t^2}{U}$ and $J_d \sim \frac{2t_d^2}{U}$ should be of the same order of magnitude. This is indeed confirmed by spin-polarized LDA + U calculations [14] where CO for the $3d$-electrons in the V-V rungs has to be assumed. They also show that CO $\alpha'-NaV_2O_5$ is in an insulating state for sufficiently large on-site $U \geq 3$ eV contrary to conventional LDA-calculations which predicts a metallic state. As a mean field like theory with broken orbital symmetry the LDA + U approach does of course not describe the true microscopic nature of the disordered MV insulating state above T_c. This is still an open problem. The transition from the high temperature MV state to the CO state was investigated in reference [8]. It was described within a frustrated 2D Ising model where the Ising spin $\tau_z = \pm 1$ denotes the $3d$-electron localized on the right or left position of the rung. In this context the CO of Figures 1a and 1b can then be described by an order parameter $\langle \tau_z \rangle_{\mathbf{Q}} = \sum_i \langle \tau_z^i \rangle \exp(i\mathbf{Q}\mathbf{R}_i)$. For $\mathbf{Q} = 0$ one obtains the "ferro-" type in-line CO structure and for $\mathbf{Q} = (\pi, \pi)$ the "antiferro-" type zig-zag CO structure depending whether $K(0) = K_1 - K_2 > 0$ or $K(\mathbf{Q}) = K_2 - K_1 > 0$. In this way model Hamiltonians of the effective Ising type as in reference [8] or extended Hubbard models in Hartree-Fock approximation [10] may be used to describe the CO transition in a qualitative way. However it is illusory to use such model Hamiltonians in an attempt to actually predict the most favorable CO structure. This requires a method like LDA + U which can provide *ab initio* (aside from U) total energies of the various CO structures. It has been successfully used for CO-phenomena in semimetallic $4f$-compounds [7] and may also be a powerful method for the vanadates [14]. In this work the CO mechanism itself is not considered. We rather start from plausible candidate structures at low temperature and an appropriate exchange model. The derivation of an exchange model for $\alpha'-NaV_2O_5$ from an original extended Hubbard model was described in reference [8] and is briefly recapitulated here. It proceeds by eliminating high energy charge fluctuations between the rungs, thus confining one d-electron or spin within each rung. Within this subspace the original model may be mapped to an effective low energy Hamiltonian containing the d-electron spin and (Ising) pseudo-spin degrees of freedom, the latter describes which of the degenerate V-positions in the rung is occupied. This Hamiltonian is formally similar to those used for the manganites where the pseudospin describes an orbital degeneracy of Mn ions. The Ising variable describes the CO transition and for $T \ll T_c$ where the intra-rung charge fluctuations are also frozen we may replace it by its expectation value, *i.e.* the CO parameter. In this way the effective Hamiltonian reduces to an effective spin exchange Hamiltonian only, however with an exchange constant J_{nm} (n, m = V-sites) that *depends* on the CO parameter, *i.e.* on the degree of charge disproportionation between the inequivalent V-atoms in $\alpha'-NaV_2O_5$. In this low temperature approximation which we use here the actual size of the CO parameter is absorbed in the exchange constants and influences *only* the energy scale of the spin dynamics, the form of the exchange Hamiltonian ($T \ll T_c$) is of the usual type as for spins in a completely CO system. In our case due to the orthorhombic symmetry it is essential to include exchange anisotropies which may be important

for small mode splittings as observed in $\alpha'-NaV_2O_5$. The model exchange Hamiltonian for the proposed CO structures in Figures 1 and 6 is then given by

$$H = \frac{1}{2}\sum_{n,m}(J^x_{nm}S^x_nS^x_m + J^y_{nm}S^y_nS^y_m + J^z_{nm}S^z_nS^z_m) \\ -g\mu_B H\sum_n S^z_n. \quad (1)$$

Here J^α_{nm} ($\alpha = x, y, z$) denotes both inter- and intra-chain couplings which may be different along the three crystal axis $\mathbf{a}, \mathbf{b}, \mathbf{c}$ (x, y, z). Note that part of the anisotropy in equation (1) may be due to a Dzyaloshinski-Moriya interaction which can be transformed away in 1D in a manner described in reference [24] and references cited therein. A Zeeman term with field direction perpendicular to the vanadium ab-planes is also included to study the field dependence of excitations. Which exchange couplings have to be used depends on the CO structure, *i.e.* the position of the V^{4+} $S = \frac{1}{2}$ spins because exchange bonds to V^{5+}-ions with no d-electrons and $S = 0$ are irrelevant for the spin dynamics. This is shown in Figures 1 and 6 with sets of intra- (J, J_d) and inter-chain (J', J'_d, J_l) exchange parameters (the Cartesian index α is suppressed). The former may be dimerized to $J_{1,2} = J(1 \pm \delta)$ (Fig. 1a) and $J_{1,2} = J_d(1 \pm \delta)$ (Fig. 1b). This set has been enlarged as compared to reference [8] where only J, J' were included. Note that J_d and J' are not contributing in the in-line CO structure of Figure 1a; J is inactive for the zig-zag structure (Fig. 1b) and J' is not relevant in the structures of Figure 6. In this work we consider the following cases. (1) Quasi-1D models either in the in-line, zig-zag or ladder CO where the inter-chain or -ladder couplings J', J'_d etc. are assumed to be much smaller than the intra-chain couplings J, J_d or the intra-ladder $\tilde{J}$. (2) A quasi-2D model where J' is of the same order as J and J_d. This possibility has been suggested by recent LDA + U results. (3) A mixed CO/MV structure which will be discussed later. Different methods have to be used for calculating the excitation spectrum in these cases. Figures 1a and 1b show that J and J_d play the same role for in-line and zig-zag quasi-1D models respectively. Therefore one has in both cases quasi-1D spin chains with intra-chain coupling J (in-line) or J_d (zig-zag) coupled by small inter-chain interactions J'_d (in-line) and J' (zig-zag). There is one essential difference however: in the in-line structure the CO-transition itself does not lead to a dimerization of the chain with an intra-chain J along $\mathbf{b}$. This may be due to a secondary SP-transition slightly below [8] leading to a dimerization $J \to J(1 \pm \delta)$ with $\delta \ll 1$. On the other hand CO in the zig-zag structure may itself be accompanied by a lattice distortion such that the two legs of the zig-zag chain have different length leading directly to a dimerized exchange $J_d(1 \pm \delta)$. However it is possible that even in this structure the most important contribution to the dimerization comes from the exchange energy J_d along the zig-zag legs in Figure 1b. Irrespective of the origin of dimerization a spin gap opens for both CO chain structures with its size $\Delta_s(\delta)$ depending on dimerization strength. On the other hand if a spin ladder structure as Figure 6a is realised in $\alpha'-NaV_2O_5$ a spin gap will appear already without dimerization along $\mathbf{b}$. Finally in the quasi-2D model with strongly coupled chains and in the mixed CO/MV model a broken symmetry spin wave (SW) calculation will show that the spin gap can be attributed to pure anisotropy effects.

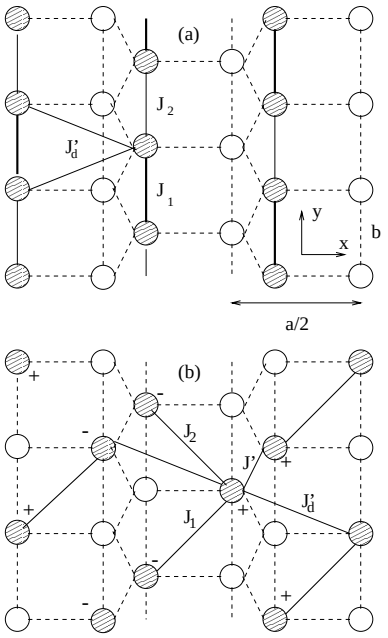

Fig. 1. Charge ordered (CO) structures of $\alpha'-NaV_2O_5$ discussed in the text. Hatched circles: V^{4+} ($S = \frac{1}{2}$), open circles: V^{5+} ($S = 0$). Oxygen atoms on the legs and rungs of V-ladders are not shown. Thick lines (J_1 or $\tilde{J}$) denote the dimer basis of each model. (a) In-line CO with active exchange constants $J_{1,2} = J(1 \pm \delta)$ and J'_d; δ = dimerization strength along b. (b) Zig-zag CO with active exchange constants $J_{1,2} = J_d(1 \pm \delta)$, J' and J'_d. The $\pm$ signs denote the spin configuration with lowest energy for the LDA + U exchange parameters. This is only relevant for the 2D spin wave scenario of Section 4.3.

For the single dimerized chain or the spin ladder methods based on the Jordan-Wigner transformation [15,16] exist to investigate the excitation spectrum. However the focus in this work is primarily on the typical behaviour of the *transverse* dispersion ($\mathbf{q} \perp \mathbf{b}^*$) of excitations where the influence of interchain coupling and exchange anisotropies has to be studied. For this purpose it is necessary to use a simple theory as starting point for the intra-chain excitations ($\| \mathbf{b}^*$). It is physically appealing to use a spin dimer representation where the presence of a spin gap is already manifest in the local dimer basis as a singlet-"triplet" splitting. This representation may also be mapped to the so called bond boson model introduced in reference [17] for spin ladders. However, for the purpose of investigating spin excitations only it is more convenient to keep the original spin-dimer basis, especially when the effect of exchange anisotropies on excitations is to be considered. The basic features of the spin-dimer representation following reference [18] are outlined in the next section and adapted to the relevant CO spin structures on the Trellis lattice.

3 The local spin dimer model

In the dimerized phase of the chain models Figures 1a and 1b or in the case of a ladder with $\tilde{J} > J$ (Fig. 6a) it is a useful approach to start from a basis where the strongest exchange pairs *i.e.* $J(1+\delta)$ or $\tilde{J}$ respectively are diagonalized exactly and the weaker couplings are treated perturbatively in random phase approximation (RPA). This method has first been used in reference [18] in a different context. Presently this means the introduction of dimer variables

$$\begin{aligned} \mathbf{K}_i &= \mathbf{S}_{1i} + \mathbf{S}_{2i} \\ \mathbf{L}_i &= \mathbf{S}_{1i} - \mathbf{S}_{2i} \end{aligned} \tag{2}$$

for each pair of strongly coupled dimer spins ($\mathbf{S}_{1i}$, $\mathbf{S}_{2i}$) where $\mathbf{R}_i$ denotes the positions in the dimer covering lattice. Using this mapping the Hamiltonian in equation (1) may be transformed to

$$\begin{aligned} H = \frac{1}{4}\sum_{i\alpha} J_1^\alpha (K_i^\alpha K_i^\alpha - L_i^\alpha L_i^\alpha) - g\mu_\mathrm{B} H \sum_i K_i^z \\ -\frac{1}{8}\sum_{\langle ij\rangle\alpha} J_2^\alpha L_i^\alpha L_j^\alpha - \frac{1}{8}\sum_{\langle\langle ij\rangle\rangle\alpha} J_3^\alpha(i,j) L_i^\alpha L_j^\alpha. \end{aligned} \tag{3}$$

Here the first and second term $\sim J_1^\alpha$ describes the local dimer energy and the Zeeman energy respectively, the third term $\sim J_2^\alpha$ denotes the n.n. dimer interactions along the chain direction **b** and the last term J_3^α interactions of dimers on different chains. For the two chain CO models we have $J_1^\alpha = J_\alpha(1+\delta)$, $J_2^\alpha = J_\alpha(1-\delta)$ (with $J_\alpha > 0$ for AF intra-chain exchange) and J_3^α depends on the specific model discussed. Since J and J_d play the same role in the in-line and zig-zag model respectively we formally identify $J_d \to J$ in subsequent discussions of these two models. For the ladder model one has $J_1^\alpha = \tilde{J}_\alpha$ and $J_2^\alpha \equiv J_e^\alpha = J_d^\alpha - J^\alpha$. In the Hamiltonian of equation (3) irrelevant parts containing terms $\sim K_i^\alpha K_j^\alpha$ and $L_i^\alpha K_j^\alpha$ are not included because they do not have matrix elements from the singlet ground state to the excited states and hence do not contribute to the dispersion of spin excitations [18]. The energies and states of the $S = \frac{1}{2}$ dimer are given by

$$\begin{aligned} E_1 &= 0 \\ E_2 &= J_1 = \frac{1}{2}(J_1^x + J_1^y) \\ E_3 &= J_1 - j_1' + j_1 = \frac{1}{2}(J_1^x + J_1^z) = \Delta' \\ E_4 &= J_1 - j_1' = \frac{1}{2}(J_1^y + J_1^z) = \Delta \\ |\psi_1\rangle &= \frac{1}{\sqrt{2}}(|\uparrow\downarrow\rangle - |\downarrow\uparrow\rangle) \\ |\psi_2\rangle &= \frac{1}{\sqrt{2}}(|\uparrow\downarrow\rangle + |\downarrow\uparrow\rangle) \\ |\psi_3\rangle &= \frac{1}{\sqrt{2}}(|\uparrow\uparrow\rangle + |\downarrow\downarrow\rangle) \\ |\psi_4\rangle &= \frac{1}{\sqrt{2}}(|\uparrow\uparrow\rangle - |\downarrow\downarrow\rangle). \end{aligned} \tag{4}$$

The ground state singlet $|\psi_1\rangle$ is separated by an energy $\sim J_1$ from the triplet states which are slightly split by an energies $j_1' - j_1$ and j_1' due to the exchange anisotropies given by $j_1 = \frac{1}{2}(J_1^x - J_1^y)$, $j_1' = \frac{1}{2}(J_1^x - J_1^z)$ where $|j_1|$, $|j_1'| \ll |J_1|$. In the isotropic case $j_1 = j_1' \equiv 0$ the excited states form a dimer triplet at $\Delta = \Delta' \equiv J_1$. The dipolar matrix elements $|M_\alpha^i|^2 = |\langle\psi_1|L_\alpha|\psi_i\rangle|^2$ calculated from equation (4) are given by $|M_y^3|^2 = |M_x^4|^2 = 1$ and zero else. Therefore in the dynamical spin susceptibility $u_{\alpha\beta}(\omega)$ of a single dimer only $E_3 = \Delta'$ and $E_4 = \Delta$ appear as possible dimer excitations which is obvious from the form of dimer states $|\psi_i\rangle$ in equation (4). For the present zero field case $u_{\alpha\beta}(\omega) = u_{\alpha\alpha}(\omega)\delta_{\alpha\beta}$ (α, $\beta = x$, y) with

$$u_{xx}(\omega) = \frac{2\Delta}{\Delta^2 - \omega^2}, \quad u_{yy}(\omega) = \frac{2\Delta'}{\Delta'^2 - \omega^2}\,. \tag{5}$$

Due to both intra- and inter-chain interactions the two local dimer excitations at Δ, Δ' will turn into dispersive propagating modes whose minimum energy is the spin gap Δ_s. Before we discuss this in detail in the next section we first investigate the effect of an external field $\parallel c$ on the dimer states described by the Zeeman term in equation (3). Because K_z commutes with $\mathbf{K}^2$ one has $\langle\psi_1|K_z|\psi_i\rangle = 0$; *i.e.* no mixing of singlet and triplet states. The only non zero matrix element is $\langle\psi_3|K_z|\psi_4\rangle$, therefore the energies $E_{1,2}$ and states $|\psi_{1,2}\rangle$ will be unchanged but $E_{3,4}$ and $|\psi_{3,4}\rangle$ become field dependent:

$$\begin{aligned} |\psi_+\rangle &= u|\psi_3\rangle + v|\psi_4\rangle \\ |\psi_-\rangle &= -v|\psi_3\rangle + u|\psi_4\rangle \\ u^2 &= \frac{h^2}{h^2 + [(j_1^2+h^2)^{\frac{1}{2}} - j_1]^2} \\ v^2 &= \frac{[(j_1^2+h^2)^{\frac{1}{2}} - j_1]^2}{h^2 + [(j_1^2+h^2)^{\frac{1}{2}} - j_1]^2}\,. \end{aligned} \tag{6}$$

The energies of the new eigenstates $|\psi_\pm\rangle$ are given by

$$\begin{aligned} E_+ = \Delta'(h) &= J_1 - j_1' + \frac{1}{2}j_1\left[1 + \left(1 + \left(\frac{h}{j_1}\right)^2\right)^{\frac{1}{2}}\right] \\ E_- = \Delta(h) &= J_1 - j_1' + \frac{1}{2}j_1\left[1 - \left(1 - \left(\frac{h}{j_1}\right)^2\right)^{\frac{1}{2}}\right]. \end{aligned} \tag{7}$$

In the limit $h \to 0 |\psi_\pm\rangle \to |\psi_{3,4}\rangle$ and $E_\pm \to E_{3,4}$. The local dimer susceptibility $u_{\alpha\beta}(\omega)$ is now given by

$$\begin{aligned} u_{xx}(\omega) &= \frac{2u^2\Delta(h)}{\Delta(h)^2 - \omega^2} + \frac{2v^2\Delta'(h)}{\Delta'(h)^2 - \omega^2} \\ u_{yy}(\omega) &= \frac{2u^2\Delta'(h)}{\Delta'(h)^2 - \omega^2} + \frac{2v^2\Delta(h)}{\Delta(h)^2 - \omega^2} \\ u_{yx}(\omega) &= -u_{xy}(\omega) = 2\mathrm{i}\omega uv\frac{\Delta(h)^2 - \Delta'(h)^2}{(\Delta(h)^2 - \omega^2)(\Delta'(h)^2 - \omega^2)}\,. \end{aligned} \tag{8}$$

The nondiagonal part is induced by the field. Equation (8) fully describes the local dimer magnetic response and is the basis for the determination of the collective excitations in the various CO structures of the Trellis lattice (Figs. 1 and 6b).

4 Collective magnetic excitations

In the previous section the effect of the largest intra-dimer exchange interaction J_1^α has been treated exactly within the single dimer subspace. The effect of inter-dimer exchange may now be treated perturbatively within random phase approximation (RPA). In this method the collective magnetic excitations of the chain or ladder system are given by the dynamical RPA susceptibility

$$\overleftrightarrow{\chi}(\mathbf{q},\omega) = [\overleftrightarrow{1} - \overleftrightarrow{J}(\mathbf{q})\overleftrightarrow{u}(\omega)]^{-1}\overleftrightarrow{u}(\omega) \equiv \overleftrightarrow{D}^{-1}(\mathbf{q},\omega)\overleftrightarrow{u}(\omega). \quad (9)$$

Here $\overleftrightarrow{u}(\omega)$ is the local dimer susceptibility tensor of equation (8) and $\overleftrightarrow{J}(\mathbf{q})$ the exchange tensor between the *dimers* which depends on the specific CO-model considered, $\mathbf{q} = (q_x, q_y)$ is a wave vector in the reciprocal a^*b^*-plane in units of $\frac{1}{a}$ and $\frac{1}{b}$. The tensors in equation (9) have double indices: Cartesian $\alpha, \beta = x, y, z$ as well as CO-sublattice $\lambda, \tau =$ A, B. Explicitly $J^{\alpha\beta}_{\lambda\tau}(\mathbf{q}) = \delta_{\alpha\beta}J^{\alpha\alpha}_{\lambda\tau}(\mathbf{q})$ and $u^{\alpha\beta}_{\lambda\tau}(\omega) = \delta_{\lambda\tau}u_{\alpha\beta}(\omega)$. For two sublattice CO-structures and two local dimer excitations Δ, Δ' with x, y polarisation one has to expect four ($\kappa = 1$–4) collective excitation branches $\omega_\kappa(\mathbf{q})$. They are given as poles of $\overleftrightarrow{\chi}(\mathbf{q},\omega)$ or zeroes of $D(\mathbf{q},\omega)$. Strictly speaking this treatment is only valid when the intra-dimer exchange is appreciably larger than the inter-dimer coupling. For example in the dimerized chain models of Figures 1a and 1b the limit $\delta \to 0$ is problematic because then $J_1 \to J_2$ *i.e.* intra- and inter-dimer exchange become equal. As shown below, equation (9) nevertheless leads to the qualitatively correct behaviour for the spin gap $\Delta_s(\delta \to 0) \to 0$ although with a different scaling exponent. This indicates that the present approach is more effective than the bond-boson theory in MF-approximation [17] which leads to a singular Δ_s for $\delta = 0$.

4.1 Excitations for single dimerized chains

To separate the effects of intra-chain exchange anisotropies from those of inter-chain or sublattice coupling it is useful to analyse first the single chain case at zero field. Then $J^{\alpha\alpha}_{\lambda\tau}(\mathbf{q}) = J^{\alpha\alpha}_D(\mathbf{q})\delta_{\lambda\tau}$ is diagonal in the dimer sublattice basis and equation (9) factorizes for x, y polarisation and only two modes exist. The resulting zeroes of $\overleftrightarrow{D}_{x,y}(\mathbf{q},\omega)$ are then the two propagating dimer excitations $\omega_{x,y}(\mathbf{q})$ where $\mathbf{q} = q\mathbf{b}^*$ is directed along the chain direction. The result applies both for the single linear chain and the zig-zag chain in Figures 1a and 1b (with renaming $J_d \to J$ implied as explained in the previous section). Using equation (5) and the appropriate $J(\mathbf{q})$ the mode dispersions are obtained as

$$\omega_x^2(q) = \frac{1}{2}(J_y + J_z)\Big[\frac{1}{2}(J_y + J_z)(1+\delta)^2 - J_x(1-\delta^2)\cos 2q\Big]$$
$$\omega_y^2(q) = \frac{1}{2}(J_x + J_z)\Big[\frac{1}{2}(J_x + J_z)(1+\delta)^2 - J_y(1-\delta^2)\cos 2q\Big]. \quad (10)$$

The spin gap $\Delta_s(\delta)$ is obtained as the minimum of $\omega_{x,y}(q)$. The x, y-mode splitting at the $q = 0$ is then given by

$$\omega_x^2(0) - \omega_y^2(0) = \frac{1}{2}(J_x - J_y)(1+\delta) \times[(1+\delta)(\Delta + \Delta') - (1-\delta)J_z] \quad (11)$$

which is proportional to the in-plane anisotropy $j_1 = \frac{1}{2}(J_x - J_y)(1+\delta)$. If $j_1 \equiv 0$ the x, y modes are degenerate which can already be seen from their corresponding local dimer excitations E_3, E_4 in equation (4). For $\delta = 0$ one has

$$\omega_x = (\Delta D_x)^{\frac{1}{2}}; \quad D_x = \frac{1}{2}[J_y + J_z - 2J_x] > 0$$
$$\omega_y = (\Delta D_y)^{\frac{1}{2}}; \quad D_y = \frac{1}{2}[J_x + J_z - 2J_y] > 0. \quad (12)$$

For the uniaxial case, using $J_z > J_x = J_y$ without loss of generality and $D_{x,y} = \frac{1}{2}[J_z - J_{x,y}]$ this leads to $\omega_{x,y} = \frac{1}{2}(J_z^2 - J_{x,y}^2)^{\frac{1}{2}} \equiv \Delta_s$. In this limit the spin gap is a pure anisotropy gap. Approaching the Heisenberg case Δ_s vanishes. It is also instructive to consider the dispersion equation (10) directly for the Heisenberg case for $\delta \geq 0$:

$$\omega_{x,y}^2 \equiv \omega^2(q) = 2J^2(1+\delta)(\sin^2 q + \delta\cos^2 q). \quad (13)$$

This leads to a spin gap given by

$$\frac{\Delta_s}{J} = (2\delta)^{\frac{1}{2}}(1+\delta)^{\frac{1}{2}}. \quad (14)$$

For $\delta \to 0$ it vanishes like $\Delta_s \sim \delta^{\frac{1}{2}}$. Thus the spin dimer RPA approximation gives again a qualitatively correct behaviour although the δ-scaling exponent $\frac{1}{2}$ is smaller than the exact one [15] which is $\frac{2}{3}$. The dispersion equation (13) reduces to

$$\omega(q) = \alpha J \sin q \quad (15)$$

for the undimerized chain with $\alpha = \sqrt{2}$. This is slightly smaller than the value $\alpha_{\mathrm{DCP}} = \pi/2$ for which equation (15) describes the lower boundary of the exact Des Cloizeaux Pearson (DCP) excitation spectrum of the 1D HAF [19]. Of course the present spin dimer theory completely misses the fact that the excitations really consist of a free two spinon continuum since it starts from local dimer excitations which could be interpreted as two spinon bound states.

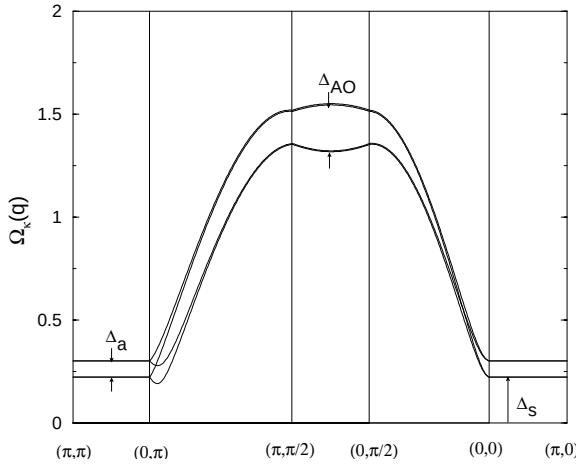

Fig. 2. Spin excitations $\Omega_\kappa(\mathbf{q}) = \omega_\kappa(\mathbf{q})/J^z$ ($\kappa = 1$–4) in the in-line structure calculated with dimer RPA-theory of equation (19). Only J^α ($\alpha = x,\ y,\ z$) and J'_d are active exchange constants, the former determines the large dispersion along $\mathbf{b}^*$ (q_y), the latter the A-O splitting $\Delta_{\rm AO}$. The spin gap Δ_s is mainly caused by the dimerization δ. J'_d has no influence along paths with $q_y = 0,\ \pi$, therefore in this model Δ_a is a pure anisotropy splitting determined by $J_x - J_y$ and the two split modes are dispersionless along q_x. In the xy-isotropic case $\Delta_a = 0$. Exchange parameters used are $J_x = 38.4$ meV, $J_y = 37.4$ meV, $J_z = 37.9$ meV, $J'_d = -6$ meV and dimerisation $\delta = 0.034$.

4.2 Excitations for weakly coupled dimerized chains, the transverse dispersion problem

The results of the last section give confidence that the basic properties of magnetic excitations in dimerized spin chains are correctly described by the dimer RPA-theory. The advantage of this approach, aside from its simplicity lies in the fact that it can easily be extended to include inter-chain coupling. These couplings may lead to transverse dispersion with $\mathbf{q} \perp \mathbf{b}^*$, *i.e.* a dependence of excitation energy on q_x in addition to the intra-chain dispersion or dependence on q_y. As mentioned previously the q_x-dispersion may give important clues about the underlying CO-structure.

First we consider the zero-field case: then again equation (9) factorizes into x, y-polarisations but now with sublattice-exchange terms for each polarisation given by ($\alpha = x,\ y$)

$$J^\alpha_{\rm AA}(\mathbf{q}) = J^\alpha_{\rm BB}(\mathbf{q}) \equiv J^\alpha_D(\mathbf{q})$$
$$J^\alpha_{\rm AB}(\mathbf{q}) = J^\alpha_{\rm BA}(\mathbf{q})^* \equiv J^\alpha_N(\mathbf{q}) \qquad (16)$$

where J^α_D, J^α_N refer to intra- and inter-sublattice exchange with A, B denoting the two inequivalent *dimer* sublattices of the CO-structures. The four magnetic excitation branches of the planar system of chains in Figures 1a and 1b are obtained as solutions of

$$1 - u_{\alpha\alpha}(\omega)[J^\alpha_D(\mathbf{q}) \pm |J^\alpha_N(\mathbf{q})|] = 0. \qquad (17)$$

The choice of $\pm$ in this equation determines the frequency of the acoustical (A) or optical (O) mode with respect to the two sublattices.

4.2.1 In-line chain structure

We first discuss the in-line CO structure of Figure 1a. It has exchange Fourier components

$$J^\alpha_D(\mathbf{q}) = \frac{1}{2} J^\alpha_2 \cos 2q_y$$
$$J^\alpha_N(\mathbf{q}) = -J'^\alpha_d \sin q_y \sin \frac{1}{2}(q_x + q_y). \qquad (18)$$

Together with equation (5) the above equations lead to the four mode dispersions

$$\omega^2_{x\pm}(\mathbf{q}) = \frac{1}{2}(J_y + J_z)\Big[\frac{1}{2}(J_y + J_z)(1+\delta)^2 - J_x(1-\delta^2)\cos 2q_y\Big] \pm (J_y + J_z) J'^x_d (1+\delta) \sin q_y \sin \frac{1}{2}(q_x + q_y)$$
$$\omega^2_{y\pm}(\mathbf{q}) = \frac{1}{2}(J_x + J_z)\Big[\frac{1}{2}(J_x + J_z)(1+\delta)^2 - J_y(1-\delta^2)\cos 2q_y\Big] \pm (J_x + J_z) J'^y_d (1+\delta) \sin q_y \sin \frac{1}{2}(q_x + q_y). \qquad (19)$$

An interesting aspect of this equation is that for $q_y = 0,\ \pi$ where the excitation energy is close to the spin gap Δ_s, there is *no* transverse dispersion for the in-line CO model along the lines $(q_x, 0)$ and (q_x, π). The dispersion of modes for the present case is shown in Figure 2, unfolded in the $(q_x,\ q_y)$-plane. The inter-chain coupling J'_d has its largest effect at the maximum mode energy along $(q_x, \frac{\pi}{2})$ where it causes an additional acoustic(A)-optic(O) mode splitting connected with the $\pm$ in the above equation and in addition it leads to a q_x-dispersion. On the other hand when $\mathbf{q} = (q_x, 0)$ or $(q_x,\ \pi)$ J'_d has no effect and the observed mode splitting in Figure 3 is dispersionless, it is not of A-O type but has pure anisotropy character as in the single chain case of equation (10).

4.2.2 Zig-zag chain structure

In Section 4.1 it was noted that for a single chain this model is equivalent to the in-line structure. However it can be seen from Figures 1a and 1b that the inter-chain coupling is different in the two models. For the in-line structure a given dimer is symmetrically coupled with $\pm\ J'_d$ to four dimers on two neighboring chains whereas in the zig-zag model the coupling is asymetric with strength $-J'_d$, $\frac{1}{2}J'$. This leads now to Fourier components for the exchange given by

$$J^\alpha_D(\mathbf{q}) = \frac{1}{2} J^\alpha_2 \cos 2q_y$$
$$J^\alpha_N(\mathbf{q}) = \frac{1}{2} J'^\alpha \cos\left(\frac{3}{2}q_y + \frac{1}{2}q_x\right) - J'^\alpha_d \cos\left(\frac{3}{2}q_y - \frac{1}{2}q_x\right). \qquad (20)$$

Using equation (17) we obtain the explicit solutions (with the formal replacement $J_d \to J$)

$$\omega^2_{x\pm}(\mathbf{q}) = \frac{1}{2}(J_y+J_z)\left[\frac{1}{2}(J_y+J_z)(1+\delta)^2 - J_x(1-\delta^2)\cos 2q_y\right] \pm (J_y+J_z)\left[J_d'^x \cos\left(\frac{3}{2}q_y - \frac{1}{2}q_x\right) - \frac{1}{2}J'^x \cos\left(\frac{3}{2}q_y + \frac{1}{2}q_x\right)\right]$$

$$\omega^2_{y\pm}(\mathbf{q}) = \frac{1}{2}(J_x+J_z)\left[\frac{1}{2}(J_x+J_z)(1+\delta)^2 - J_y(1-\delta^2)\cos 2q_y\right] \pm (J_x+J_z)\left[J_d'^y \cos\left(\frac{3}{2}q_y - \frac{1}{2}q_x\right) - \frac{1}{2}J'^y \cos\left(\frac{3}{2}q_y + \frac{1}{2}q_x\right)\right]. \quad (21)$$

While the intra-chain part in this expression is the same as in the in-line model of equation (10) the second part leading to the transverse q_x-dispersion is completely different. For example taking $q_y = \pi$ we obtain

$$\omega^2_{x-}(q_x,\pi) - \omega^2_{x+}(q_x,\pi) = \left(J_d'^x + \frac{1}{2}J'^x\right)(J_y+J_z)\sin\frac{1}{2}q_x$$

$$\omega^2_{y-}(q_x,\pi) - \omega^2_{y+}(q_x,\pi) = 2\left(J_d'^y + \frac{1}{2}J'^y\right)(J_x+J_z)\sin\frac{1}{2}q_x. \quad (22)$$

This shows that in addition to the anisotropy induced x, y-mode splitting each of them shows a further splitting into A, O ($\pm$)-modes which has dispersion: it vanishes at $q_x = 0$ and is at maximum for $q_x = \pi$. This situation is clearly illustrated in Figure 3. Whether this dispersion is visible in the experiment depends on how large it is against the pure anisotropy splitting caused by the intra-chain exchange. In principle both are present and Figure 3b shows two typical possibilities. The q_x *dispersive* A-O splitting which is absent for $q_y = 0$, π in the in-line case therefore in principle offers a possibility to distinguish between both models.

Finally we discuss the intensity variation of $q_y = 0$, π spin gap modes as function of total momentum transfer $\kappa = \mathbf{q} + \boldsymbol{\tau}(\mathbf{q} \in 1.\mathrm{BZ})$ mentioned in reference [11]. It was observed that the intensity of the $\hbar\omega = 10$ meV excitation exhibits unexpected variation in τ_x with period $h = 3$ where $\boldsymbol{\tau} = (2\pi h, 2\pi k, 0)$ is a reciprocal lattice vector in the ab-plane. For a strictly 1D system the intensity should rather be constant and therefore this variation possibly points to a more 2D character of magnetic excitations. We now analyze the intensities in the dimer RPA model for that structure. For simplicity we neglect the additional splitting of modes caused by xy-exchange anisotropy, *i.e.* we assume $J_x = J_y$. Then the observed splitting along q_x is entirely an A-O splitting due to the fact that the *dimer* lattice consists of two sublattices. In this case the intensities

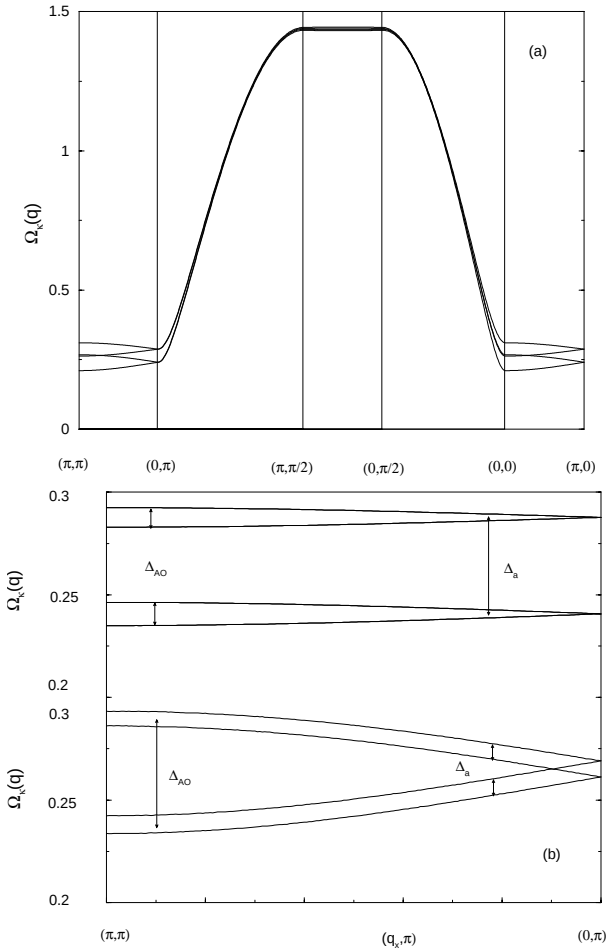

Fig. 3. Spin excitations $\Omega_\kappa(\mathbf{q}) = \omega_\kappa(\mathbf{q})/J_d^z$ ($\kappa = 1{-}4$) in the zig-zag CO structure according to equation (19) (where the formal replacement $J_d \to J$ was made). Only J_d^α, J' and J_d' (Fig. 1b) are active exchange constants in this structure. (a) In addition to the anisotropy splitting Δ_a along q_x there is a further A-O splitting superposed. Which one is more pronounced depends on the relative size of xy-anisotropy $J_d^x - J_d^y$ and the inter-ladder coupling J'. In this plot $J_d^x = 38.2$ meV, $J_d^y = 37.6$ meV, $J_d^z = 37.9$ meV, $J' = 0.5$ meV, $J_d' = 0$ and $\delta = 0.034$ was used. (b) Enlarged excitation branches between (π,π) and $(0,\pi)$ for two extreme cases. above: large anisotropy $J_d^x = 38.2$ meV, $J_d^y = 37.6$ meV, $J_d^z = 37.9$ meV and small $J' = 0.1$ meV. Below: small anisotropy $J_d^x = 37.95$ meV, $J_d^y = 37.85$ meV, $J_d^z = 37.9$ meV and large $J' = 0.5$ meV. Other parameters in both cases as in (a). It is seen that anisotropy splitting Δ_a and A-O splitting Δ_{AO} interchange roles in the two cases. The situation proposed previously [11] corresponds more to the lower part. Parameters for the dispersion in (a) are between these two extreme cases.

may be obtained from the dynamical susceptibilities [20] decomposed according to

$$\overleftrightarrow{\chi}(\mathbf{q}+\boldsymbol{\tau},\omega) = \frac{1}{2}(1+\cos\Phi)\overleftrightarrow{\chi}_{\mathrm{A}}(\mathbf{q},\omega) + \frac{1}{2}(1-\cos\Phi)\overleftrightarrow{\chi}_{\mathrm{O}}(\mathbf{q},\omega) \quad (23)$$

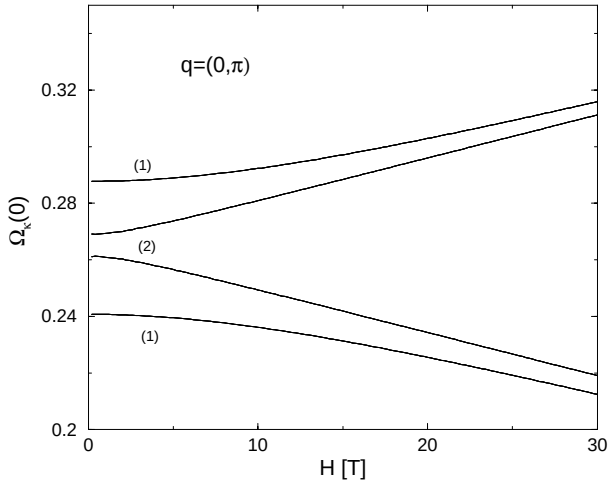

Fig. 4. Field dependence of modes at $\mathbf{q} = (0,\ \pi)$ for the zig-zag CO. Exchange parameters for (1) and (2) are identical to those of the upper and lower part of Figure 3b respectively.

where $\phi = \boldsymbol{\tau} \cdot \boldsymbol{\rho}$ and $\boldsymbol{\rho} = (\frac{1}{2}, -\frac{1}{2})$ is the vector joining the two *dimer* sublattices in units of a, b respectively (Fig. 1b) which leads to $\Phi = h\pi - k\pi$. From the imaginary part of $\chi(\mathbf{q}, \omega)$ the A, O intensities are obtained as ($\mathbf{q} \in$ 1.BZ)

$$I_{\mathrm{A,O}}(\mathbf{q} + \boldsymbol{\tau}) = \frac{\Delta}{2\omega_{\mathrm{A,O}}(\mathbf{q})}[1 \pm \cos(h\pi - k\pi)] \qquad (24)$$

where $\pm$ corresponds to A, O respectively. In the experiments [11] one has $\mathbf{q} = (q_x, \pi)$ and $\boldsymbol{\tau}$ given by $(2\pi h, 0)$. Neglecting the small A-O splitting, *i.e.* setting $\omega_{\mathrm{A,O}}(\mathbf{q}) \simeq \Delta_s$ one then has

$$I_{\mathrm{A,O}}(\boldsymbol{\tau}) = \frac{\Delta}{2\Delta_s}(1 \pm \cos h\pi). \qquad (25)$$

Two points are worth noting. The period of the intensity is given by $h = 2$ and not $h = 3$. The intensity maxima of slightly split A, O-modes are shifted by one half period ($h = 1$). Experimentally the intensity at an energy transfer $\hbar\omega = 10$ meV was measured as function of h. Since this energy is just in between upper (O) and lower (A) mode and both have a line width considerably higher than their splitting the measured intensity is then the *average* of A and O mode intensity. According to equation (25) however the average is a constant independent of h, irrespective of the period of individual A, O intensities. We conclude that the zig-zag CO structure, at least in the dimer RPA model for weakly coupled zig-zag chains, does neither explain the observed intensity variation nor its period.

4.2.3 Field dependence of excitations

Investigation of the field dependence of magnetic excitations may give further information on the nature of the spin gap and its observed splitting and transverse dispersion. The field dependence may also be calculated from the basic equation (9) where it enters through the local dimer susceptibility equation (8). Due to breaking of time reversal symmetry there is now a nondiagonal term $u_{xy} = -u^*_{yx}$ and both polarisations couple to each of the $\Delta(h)$, $\Delta'(h)$ local dimer transitions. The poles of equation (9) are then given by

$$1 - [u_{xx}(\omega)J^x_\pm(\mathbf{q}) + u_{yy}(\omega)J^y_\pm(\mathbf{q})] + [u_{xx}(\omega)u_{yy}(\omega) - |u_{xy}(\omega)|^2]J^x_\pm(\mathbf{q})J^y_\pm(\mathbf{q}) = 0. \qquad (26)$$

Here $J^\alpha_\pm(\mathbf{q}) = J^\alpha_D(\mathbf{q}) \pm J^\alpha_N(\mathbf{q})$ and $\pm$ has to be taken synchronously at all positions. After straightforward but lengthy algebra the solution of this equation leads to the field dependent dispersions for the magnetic excitation branches $\omega_\kappa(\mathbf{q}, h)$ ($\kappa = 1{-}4$):

$$\begin{aligned}
\omega^2_\kappa(\mathbf{q}) &= \frac{1}{2}B_\sigma \pm \frac{1}{2}[B^2_\sigma(\mathbf{q}, h) - 4C_\sigma(\mathbf{q}, h)]^{\frac{1}{2}} \\
B_\pm(\mathbf{q}, h) &= \Delta^2(h) + \Delta'^2(h) \\
&\quad - 2[\Delta(h)J^x_\pm(\mathbf{q}) + \Delta'(h)J^y_\pm(\mathbf{q})]u^2 \\
&\quad - 2[\Delta(h)J^y_\pm(\mathbf{q}) + \Delta'(h)J^x_\pm(\mathbf{q})]v^2 \\
C_\pm(\mathbf{q}, h) &= \Delta^2(h)\Delta'^2(h) \\
&\quad - 2[\Delta(h)J^y_\pm(\mathbf{q}) + \Delta'(h)J^x_\pm(\mathbf{q})]\Delta(h)\Delta'(h)u^2 \\
&\quad - 2[\Delta(h)J^x_\pm(\mathbf{q}) + \Delta'(h)J^y_\pm(\mathbf{q})]\Delta(h)\Delta'(h)v^2 \\
&\quad + 4J^x_\pm(\mathbf{q})J^y_\pm(\mathbf{q})[(\Delta^2(h) + \Delta'^2(h))u^2v^2 \\
&\quad + \Delta(h)\Delta'(h)(u^4 + v^4)]. \qquad (27)
\end{aligned}$$

Here $\sigma = \pm$ and $\kappa = (\pm, \sigma)$ corresponds to any of the four possible combinations of $\pm$-signs in the last equation. In the quantities $B_\pm$ and $C_\pm$ the $\pm$ signs always have to be taken simultaneously. With $u(h)$ and $v(h)$ given by equation (6) and $\Delta(h)$, $\Delta'(h)$ by equation (7) the above expressions represent the complete solution for the field dependent dispersion of magnetic excitations in the anisotropic coupled dimer system. These equations can be applied to the CO structures of Figures 1 and 6a. The specific CO determines only the exchange functions $J^\alpha_\pm(\mathbf{q})$. For zero field this equation reduces to the previously studied solutions of equation (17). Figure 4 shows the field dependence of $\mathbf{q} = (0, \pi)$ modes, *i.e.* the spin gap modes *vs.* external field for the zig-zag CO in the two limiting cases corresponding to Figure 3b. One obtains a quasi-linear Zeeman splitting of $\mathbf{q} = (0, \pi)$ modes in the small anisotropy (2) case and almost field independent modes for large anisotropy (1). The gap will close only at a very high field which is expected since the zero field spin gap of $\Delta_s = 10$ meV is quite large. In this model it was assumed that the dimerization δ itself shows little field dependence since it should be a direct consequence of the lattice superstructure induced by the CO.

As in the zero field case the susceptibility $\overleftrightarrow{\chi}(\mathbf{q}, \omega)$ in equation (9) may also be used to calculate the intensity of the four $\omega_\kappa(\mathbf{q}, h)$ excitation branches. They are given by the imaginary part $\pi^{-1}\chi^\perp(\mathbf{q}, \omega)''$ where $\chi^\perp = \frac{1}{2}(\chi_{xx} + \chi_{yy})$. One obtains delta-function contributions of the type $Z_\kappa\delta(\omega - \omega_\kappa(\mathbf{q}))$. The intensity of each mode $\omega_\kappa(\mathbf{q}, h)$ can

be obtained from equation (26) as

$$Z_\kappa(\mathbf{q},h) = \pm\left(\frac{\Delta+\Delta'}{2\omega_\pm}\right)\left(\frac{\omega_\pm^2 - \frac{1}{2}\gamma\frac{J_\pm^x(\mathbf{q})+J_\pm^y(\mathbf{q})}{\Delta+\Delta'}}{\omega_+^2-\omega_-^2}\right)$$
$$\gamma = 4[(\Delta^2(h)+\Delta'^2(h))u^2v^2+\Delta(h)\Delta'(h)(u^4+v^4)]. \quad (28)$$

In the isotropic case with $J_\pm^x = J_\pm^y$ and $\Delta(h) = \Delta'(h)$ this reduces to a simple formula for the two (A, O) modes ($\sigma = \pm$): $Z_\sigma(\mathbf{q},h) = \Delta(h)/\omega_\sigma(\mathbf{q},h)$ which corresponds to the prefactor of the zero field result in equation (25), the variation with $\boldsymbol{\tau}$ is suppressed here. Within the field range of Figure 4 there is only a few per cent change of the corresponding mode intensity.

4.3 Excitations in strongly coupled chains

One reason for focusing on 1D chain models for the magnetic excitations of $\alpha'-NaV_2O_5$ was the observation of quasi-1D temperature dependence of the susceptibility in the MV phase above T_c. This was attributed to d-electrons localised in the molecular bonding orbitals of each V-V rung having strong exchange J along the ladder and weak exchange J' between them. This picture was qualitatively supported by by LDA-calculations [5] mapped on an effective 3d-tight binding (TB) model which lead to very small hopping matrix elements $t' \ll t$ suggesting that $J' = \frac{4t'^2}{U} \ll J = \frac{4t^2}{U}$ in a simple superexchange picture. However a recent LDA + U analysis [14] with a mapping to an extended TB-model including both V3d and O2p orbitals has seriously questioned this picture for the low temperature CO phases. In this calculation the mapping of LDA + U total energies of various CO and spin polarized states to that of a corresponding Heisenberg model enables one to calculate realistic values for the most important exchange constants. It turns out that in the CO phase J' is only about a factor of two smaller than J_d and this "diagonal" ladder exchange is even bigger than the exchange J along the leg of the ladder. Furthermore surprisingly even the J_d' exchange constant is not negligible and both J' and J_d' are ferromagnetic. For a realistic value of $U = 3$ eV the exchange constants have values as given in the caption of Figure 5. The reason for the large J' in the CO structure as compared to the homogeneous MV state lies in the change of pd-hybridisation due to the shift of 3d-levels on inequivalent V-atoms [14]. If this LDA + U result for the exchange corresponds to the real situation then CO $\alpha'-NaV_2O_5$ is magnetically more like a 2D system with strong AF coupling along the ladder diagonals and legs and almost equally strong FM coupling between the ladders. Such a model is very different in principle from the 1D models discussed sofar. We now also investigate its magnetic excitations and origin of the spin gap which is different from the dimerization mechanism in this model. This is also partly motivated by the fact that according to reference [21] there is indeed no intra-chain dimerisation in the low temperature

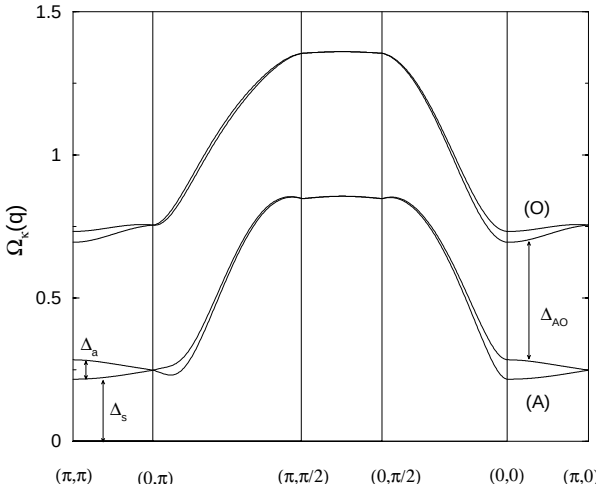

Fig. 5. Spin excitations for the 2D exchange scenario described in Section 5. The SW results of equation (33) has been used. The exchange parameters are basically those from LDA + U calculations ($U = 3$ eV) [14] for the spin polarized zig-zag CO structure of Figure 1b, except for a slightly larger J_d' and the additional anisotropies which have been introduced to obtain spin gap Δ_s and anisotropy splitting Δ_a. Explicitly we use $J_d^x = 34.5$ meV, $J_d^y = 35.2$ meV, $J_d^z = 36.2$ meV, $J' = -17.8$ meV, $J_d' = -6$ meV. In the SW picture the dimerization does not lead to a spin gap and was set to zero. Δ_s is mainly determined by the (xy)-z anisotropy and Δ_a by the in-plane xy-anisotropy. The large Δ_{AO}-gap is caused by the large J' in this parameter set.

structure as assumed in the previous models. Naturally the dimer approach of previous sections is not possible for the zig-zag CO structure with its very large interchain coupling J'. On the other hand there is no problem for the in-line structure since J' is inactive in this case and even the appreciable J_d' obtained from LDA + U does not affect the dispersion very much since it is effective only at the maximum energy and does not influence the spin gap as shown in Figure 2. For the zig-zag CO instead we now start from a broken symmetry ground state with a spin configuration as indicated in Figure 1b which has the lowest ground state energy $E = \frac{J'}{8} - \frac{J_d'}{4} - \frac{J_d}{4}$. Of course this approach does not describe the real ground state of $\alpha'-NaV_2O_5$ which is nonmagnetic, nevertheless the excitation spectrum can be expected to have realistic features. The spin state consists of four magnetic sublattices A↑, B↑, A↓, B↓. The molecular field for the sublattices λ is given by $\Delta(\uparrow) = -\Delta(\downarrow) \equiv \Delta$ with

$$\Delta = \langle S\rangle[J'^z - 2J_d'^z - 2J_d^z]. \quad (29)$$

As in the previous models we include anisotropies in the largest exchange J_d^α although its magnitude has not yet been calculated in LDA + U which was applied without spin-orbit coupling [14]. Without loss of generality we assume that the spins are oriented along the c-axis, *i.e.* $J_d^z > J_d^{x,y}$. Furthermore $\langle S\rangle$ is the saturation moment equal to 1/2 at $T = 0$. The RPA equation for the spin wave (SW) modes is formally the same as equation (9)

but the dynamical variables are now the individual spins and not the dimer excitations. Therefore instead of equation (5) for the dynamical suscepibilities we have now $u_{xx}(\omega) = u_{yy}(\omega) \equiv u(\omega)$ and $u_{yx}(\omega) = u_{xy}(\omega)^* \equiv v(\omega)$ with

$$u(\omega) = \frac{\langle S\rangle_\lambda \Delta_\lambda}{\Delta_\lambda^2 - \omega^2} \quad v(\omega) = \mathrm{i}\frac{\langle S\rangle_\lambda \omega}{\Delta_\lambda^2 - \omega^2} \tag{30}$$

where $\langle S\rangle_\lambda = \pm\langle S\rangle$ and $\Delta_\lambda = \pm\Delta$ for $\lambda = \uparrow, \downarrow$ sublattices. Furthermore the exchange Fourier transforms $\overleftrightarrow{J}^{\alpha}_{D,N}(\mathbf{q})$ ($\alpha = x, y, z$) are now tensors defined in the original spin lattice ($\uparrow, \downarrow$ sublattices) instead of the dimer covering lattice. The various components connecting the four sublattices can be read off from Figure 1b, *e.g.* $J_{D\uparrow\uparrow} = J'(\mathbf{q})$ etc. with

$$\begin{aligned} J'(\mathbf{q}) &= J' \exp \mathrm{i}\frac{1}{2}\left(\frac{1}{3}q_x - q_y\right) \\ J'_d(\mathbf{q}) &= 2J'_d \cos\frac{1}{2}(q_x + q_y) \\ J_d(\mathbf{q}) &= 2J_d \exp\left(-\frac{1}{3}q_x\right)[\cos q_y - \mathrm{i}\delta \sin q_y]. \end{aligned} \tag{31}$$

Here $\delta \ll 1$ is the dimerization of the zig-zag chain which may exist due to the low symmetry of the corresponding CO structure. After some algebra the complete RPA spin wave solution of equation (9) applied to the present case consists of four branches ($\kappa = 1$–4) which are given by $\hat{\omega}_\kappa = \omega_\kappa/\langle S\rangle$ with

$$\begin{aligned} \hat{\omega}^2_\kappa(\mathbf{q}) &= (c'_1 \hat{\pm} d'_1) \\ &\quad \pm \big\{(c'_1 \hat{\pm} d'_1)^2 - [|c_1|^2 + |d_1|^2 - |c_2|^2 - |d_2|^2 \\ &\quad \hat{\pm}(c_1 d_1^* + c_1^* d_1 - c_2 d_2^* - c_2^* d_2)]\big\}^{\frac{1}{2}} \\ c_1 &= \hat{\Delta}^2 + J'^x J'^{y*} - (J'^x_d J'^y_d + J^x_d J^{y*}_d) \\ c_2 &= -\hat{\Delta}(J'^x + J'^y) - (J^x_d J'^y_d + J^y_d J'^x_d) \\ d_1 &= \hat{\Delta}(J'^x_d - J'^y_d) + J'^x J^{y*}_d - J'^{y*} J^x_d \\ d_2 &= \hat{\Delta}(J^x_d - J^y_d) + J'^x J'^y_d - J'^y J'^x_d. \end{aligned} \tag{32}$$

Here $\hat{\Delta} = \Delta/\langle S\rangle$ and $c'_1 = (c_1 + c_1^*)/2$, $d'_1 = (d_1 + d_1^*)/2$ denotes the real part of these functions. Note that the variable $\mathbf{q}$ was suppressed in $J'(\mathbf{q})$, $J'_d(\mathbf{q})$ and $J_d(\mathbf{q})$ in the above expressions for simplicity. The signs $\hat{\pm}$ with a hat have to be taken simultaneously with upper or lower value wherever they appear thus leading to four spin wave branches. Again it is useful to consider the solutions for the single chain case only, *i.e.* setting $J' = J'_d \equiv 0$. Then equation (32) reduces to $\hat{\omega}^2_\kappa = c'_1 \pm |d_2|$ or

$$\begin{aligned} \hat{\omega}^2_\pm(\mathbf{q}) &= [\hat{\Delta} \hat{\pm} 2J^x_d \gamma_\mathbf{q}][\hat{\Delta} \hat{\mp} 2J^y_d \gamma_\mathbf{q}] \\ \gamma_\mathbf{q} &= (\cos^2 q_y + \delta^2 \sin^2 q_y)^{\frac{1}{2}}. \end{aligned} \tag{33}$$

Each branch is twofold degenerate since there is no A-O splitting without inter-chain coupling. At zero wave vector one has for $J_d > 0$, using $2\langle S\rangle = 1$:

$$\begin{aligned} \omega_+(0) &= [J^z_d - J^x_d]^{\frac{1}{2}}[J^z_d + J^y_d]^{\frac{1}{2}} \simeq (2j^x_d \bar{J}_d)^{\frac{1}{2}} \\ \omega_-(0) &= [J^z_d + J^x_d]^{\frac{1}{2}}[J^z_d - J^y_d]^{\frac{1}{2}} \simeq (2j^y_d \bar{J}_d)^{\frac{1}{2}} \end{aligned} \tag{34}$$

with $j^{x,y}_d = J^z_d - J^{x,y}_d$ and $\bar{J}_d = (J^x_d + J^y_d + J^z_d)/3$ denoting the exchange anisotropy and average respectively.

This shows that in the SW approximation the spin gap $\Delta^\alpha_s = (2j^\alpha_d \bar{J}_d)^{\frac{1}{2}}$ is entirely an anisotropy gap and independent of CO induced dimerization. Indeed in the isotropic case $\omega(\mathbf{q}) = 2\langle S\rangle J_d(1-\delta^2)^{\frac{1}{2}} \sin q_y$. The dimerization does not remove the gapless excitations but only changes slightly the spinwave velocity. Therefore not surprisingly for isolated *dimerized* isotropic HAF chains the SW RPA approximation is qualitatively incorrect and the dimer RPA approach of previous sections should be used. However when interchain couplings J', J'_d become larger than $J_d\delta$ the situation is reversed and the SW approximation of equation (32) is a better starting point for the essentially 2D magnetic system. This is certainly the case when one uses the exchange parameters obtained from LDA + U where due to $|J'/J_d| \simeq 0.5J'$ is much larger than $J\delta$ with a $\delta = 0.034$ estimated from the spin gap in the dimer model.

The SW excitation branches for the 2D exchange model as obtained from the LDA + U parameters are shown in Figure 5. The size of the anisotropy which is not determined by LDA + U is fixed by the size of the spin gap of $\simeq 10$ meV as suggested by equation (34). For zero anisotropy one would get a Goldstone mode (A-branch) also for the 2D model. Thus the anisotropy and not the CO induced dimerization of the J_d exchange is the origin of the spin gap in this 2D model. Figure 5 exhibits a pair of two strongly split A, O modes where the splitting is approximately given by $[J'(J' - 2J_d)]^{\frac{1}{2}}$. Both modes show a small additional splitting caused by the xy-exchange anisotropy of J^α_d; if it vanishes the A and O modes are twofold degenerate throughout the BZ. This fact is well known already from the simple (two magnetic sublattice) AF where only A modes exist and the degeneracy can simply be understood as a result of the downfolding into the AF BZ. The A-modes are nearly dispersionless along q_x because the effect of the AF J_d and the FM J'_d nearly cancel along this direction. The behaviour of the A-modes around the $(0, \pi)$-point with their splitting increasing towards (π, π) is qualitatively very similar to the two modes in the dimer model with weakly coupled chains (Figs. 2 and 3). Note however that the role of A-O splitting and anisotropy splitting are reversed. It is the latter which now leads to the dispersion of the small A-mode splitting whereas the A-O splitting is now much larger. The existence of the high energy split- off O-branch is an essential prediction of this 2D model and could be tested directly experimentally. The flat part of the O-branch lies at about an energy given by $\omega_\mathrm{O} \simeq [J'(J' - 2J_d)]^{\frac{1}{2}} \simeq 30$ meV roughly twice the maximum energy investigated so far [11].

4.4 Excitations in Ladder and partly mixed valent structures

Recently a model for the lattice distortion caused by the charge ordering below T_c has been proposed based on low temperature X-ray scattering [21]. According to

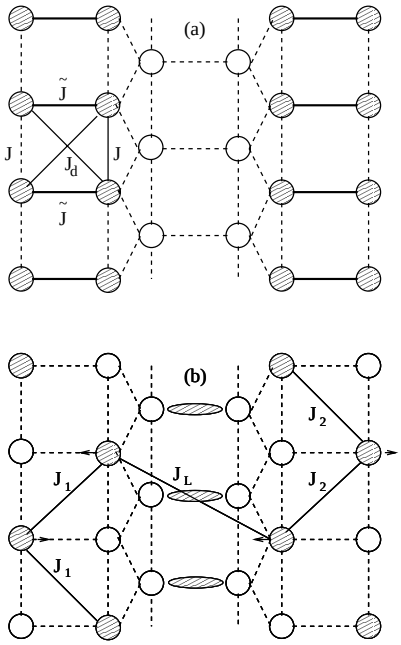

Fig. 6. (Partly) charge ordered (CO) structures of $\alpha'-NaV_2O_5$ discussed in Section 4.4. Hatched circles: V^{4+} ($S = \frac{1}{2}$), open circles: V^{5+} ($S = 0$). Hatched ellipse: $V^{4.5+}$ MV state of V-V rung. Oxygen atoms on the legs and rungs of V-ladders are not shown. (a) Ladder CO consisting of isolated $S = \frac{1}{2}$ ladders with active exchange constants J, $\tilde{J}$ and J_d. (b) Partly zig-zag CO/MV structure. Intra-chain exchange $J_{1,2} = J_d(1 \pm \delta)$ is dimerized *perpendicular* to the chain under the assumption of the low temperature distortion pattern (arrows) proposed in reference [21]. Next neighbor chains are coupled by J_l. The hatched ellipse denote one d-electron in the molecular state of the rung, *i.e.* the V-atoms have formal valence 4.5. A similar CO structure (symmetric to the MV ladder) is also possible where the CO pattern on the right ladder is shifted along **b** (chain direction) by one rung. Exchange path for J_l is then perpendicular to **b**.

this model only every second ladder in Figure 1c is distorted *perpendicular* to the chain (**b**-) direction with a period of $2a$ along the (**a**-) direction. It is not immediately obvious which CO structure is compatible with this distortion pattern but the simple in-line and zig-zag model cannot easily be reconciled with the curious fact that every second V-ladder of the Trellis lattice is undistorted. Two possible models which incorporate this fact have been proposed and are shown in Figure 6. (i) CO structure of the spin ladder type [21,22] where *two* V($3d$) electrons occupy every second rung and the other rungs have no V($3d$) electrons. This ladder model is therefore completely different from the chain models which have only *one* $3d$-electron for every rung. It seems rather surprising that the ladder structure should be realized since LDA + U calculations [14] indicate that it has a much higher total energy than the chain structures. (ii) Structure with alternating CO zig-zag chains and disordered chains [23]. Here half of the ladders have zig-zag CO like in Figure 1b but the other half remains in the disordered mixed valent state. This is again a structure with only one d-electron per rung on the average and therefore it will have a total energy not too different from the CO structure of Figure 1b.

We discuss first the magnetic excitations in the ladder structure in qualitative terms assuming an AF superexchange $\tilde{J}^\alpha$ of spins within the ladder rungs *via* the intervening oxygen. In this structure there is no connection between the spin gap and the doubling of periodicity along b since it appears already in the undimerized (equidistant) ladder. Essentially one deals with single ladder excitations in this case because the magnetic $S = \frac{1}{2}$ V^{4+} ladders are separated by nonmagnetic $S = 0$ (V^{5+}) ladders. There is another important difference to the chain structures: the doubling of the periodicity of the lattice (period $2b$) does not show up in the spin ladder which still has periodicity b as seen in Figure 1c, this has drastic consequences for the excitations. In the present case the local dimer susceptibility is determined by the states of the rung-dimer with interaction $\tilde{J}^\alpha$ (Fig. 1c) and it may be obtained by replacing $\Delta \to \frac{1}{2}(\tilde{J}^y + \tilde{J}^z)$ and $\Delta' \to \frac{1}{2}(\tilde{J}^x + \tilde{J}^z)$ in equation (5). Using equation (17) which also holds for the present case we obtain for the two excitation branches (there is no A-O splitting in this case):

$$\omega_x^2(\mathbf{q}) = \frac{1}{2}(\tilde{J}_y + \tilde{J}_z)\left[\frac{1}{2}(\tilde{J}_y + \tilde{J}_z) - 2J_e^x \cos q_y\right]$$
$$\omega_y^2(\mathbf{q}) = \frac{1}{2}(\tilde{J}_x + \tilde{J}_z)\left[\frac{1}{2}(\tilde{J}_x + \tilde{J}_z) - 2J_e^y \cos q_y\right]. \quad (35)$$

The most important aspect of these excitations is the doubling of the periodicity 2π along the ladder instead of π for the chain models. In the latter the points $q_y = 0$ and $q_y = \pi$ are degenerate and their excitation energy is at (or close) to the minimum, *i.e.* equal to the spin gap (Figs. 2 and 3). On the other hand for the ladder structure assuming $J_e^\alpha = J_d^\alpha - J^\alpha < 0$ the excitation energy is equal to the spin gap only for $q_y = \pi$, whereas it is at the maximum in the zone center (q_y=0) for AF effective inter-(rung) dimer exchange J_e. The possibility of the spin ladder model can therefore in principle be directly experimentally investigated. Finally the splitting along the transverse q_x direction will be constant and determined by the exchange anisotropy as in the in-line chain case.

The more recent proposal [23] of an alternating CO/MV low temperature structure of $\alpha'-NaV_2O_5$ which is shown in Figure 6b is a very interesting possibility and deserves a detailed analysis of its magnetic excitation spectrum. In this structure CO zig-zag chains alternate with ladders in the MV state along the a-axis. In both we have one d-electron per rung on the average but in the MV ladders the electron is not localised on one of the two V-positions of the rung but resonates, *i.e.* it is in the molecular bonding state of the two V-atoms. This means there are three types of V-sites with formal valencies $Z = 4$ or 5 on the CO zig-zag chain and $Z = 4.5$ on the MV ladder. Whether the existence of three inequivalent V-sites is compatible with NMR results [12] is not clear. To describe the magnetic excitations in such an inhomogeneous state we make a drastic but reasonable assumption.

Since the d-electrons residing in the molecular orbitals are spread out over the whole rung, their spin response will be concentrated around zero total momentum transfer contrary to the atomic spins on the CO zig-zag chains where the magnetic scattering intensity varies with the *atomic* form factor. Therefore the contribution of the spins in the molecular orbitals to the scattering cross section should be negligible at large momentum transfer and consequently *only the atomic* spins residing on the zig-zag chains will be included in the model exchange Hamiltonian for the structure of Figure 6b. This model Hamiltonian has only two (in general anisotropic) exchange constants: intra-chain J_d^α similar as in the zig-zag model of Figure 1b and inter-chain coupling J_l^α which connects V^{4+} spins on next nearest ladders *via* a superexchange path across the intervening MV (non-magnetic) ladder. Note that in principle the lattice distortion in which was described in the beginning of this section implies a dimerization $J_{1,2} = J_d(1 \pm \delta)$ of the intra-chain J_d^α *along the* **a**-*direction*. This means that the intra-chain exchange within a given zig-zag chain is $J_d(1+\delta)$ and $J_d(1-\delta)$ on two adjacent zig-zag chains separated by a MV ladder (Fig. 6b). This type of dimerization therefore leads to a doubling of the unit cell of the exchange Hamiltonian along **a** whose consequences we will discuss later. Note that it does *not* lead to an alternating exchange within a given zig-zag chain and hence *not* to a dimerization gap in the excitations of the isolated chain. For this reason it is possible to start from a Néel ground state and use the spin wave approximation even though we consider now weakly coupled zig-zag chains. Formally the SW-calculation is very similar to that performed in Section 4.3 and we do not repeat the details. The Fourier components of the exchange entering the dynamical susceptibility $\chi(\mathbf{q},\omega)$ may be read off from the structure in Figure 6b and are given by

$$J_d^\alpha(\mathbf{q}) = 2J_d^\alpha \cos q_y \exp\left(\frac{\mathrm{i}}{3}q_x\right)$$
$$J_l^\alpha(\mathbf{q}) = 2J_l^\alpha \cos q_y \exp\left(\frac{2\mathrm{i}}{3}q_x\right). \qquad (36)$$

The spin wave branches are then again obtained from the poles of $\chi(\mathbf{q},\omega)$ which leads to the secular equation $\det\chi(\mathbf{q},\omega) = 0$. In this equation the dimerization $\delta(\| \mathbf{a})$ appears only in $O(\delta^2)$ and if these terms are neglected for the moment we obtain the four spin wave branches in the small BZ ($|q_x| \le \frac{\pi}{2}$) as

$$\omega_\kappa^2(\mathbf{q}) = [(J_d^{z2} - J_d^x J_d^y) + J_d^x J_d^y \sin^2 q_y] \pm J_d^z(J_d^y - J_d^x)\cos q_y \pm J_l(J_d^x + J_d^y)\cos^2 q_y \cos q_x. \qquad (37)$$

Here $\pm$ signs are chosen independently and therefore $\kappa = 1{-}4$. For the isolated chain with uniaxial exchange ($J_l = 0$, $J_d^x = J_d^y \equiv J_d$) this reduces to a single dispersion

$$\omega^2(q_y) = \Delta_a^2 + J^2 \sin^2 q_y \qquad (38)$$

with the Ising anisotropy spin gap $\Delta_a^2 = (J_d^{z2} - J_d^2) \simeq 2J_d^z(J_d^z - J_d)$. In the Heisenberg case Δ_a=0 and one obtains the dispersion equation (15) but now with $\alpha_{\mathrm{SW}} = 1$ which is smaller than the values of α in the dimer approximation and in the exact result (see below Eq. (15)). For $J_d^x \neq J_d^y$ there are two anisotropy gaps $\Delta_a^\pm$.

We now focus on the most interesting part of the transverse dispersion along q_x of the coupled chain system. For $q_y = 0$ (or $q_y = \pi$, this leads only to an interchange of modes) one obtains in the *large* BZ ($|q_x| \le \pi$) *two unfolded* modes given by

$$\omega_+(q_x) = \Delta_a^+ - \delta^+ \cos q_x$$
$$\omega_-(q_x) = \Delta_a^- - \delta^- \cos q_x \qquad (39)$$

with $\Delta_a^{\pm 2} = 2J_d^z(J_d^z - J_d^{x,y})$ and $\delta^\pm = (J_d J_l)/\Delta_a^\pm$. In deriving equation (39) from to equation (37) we assumed that $\delta^\pm \ll 1$. These spin wave dispersions are equivalent to the recently proposed empirical dispersion relations [22] obtained by new inelastic neutron scattering results which had much higher resolution than those performed in reference [11]. The above formulas provide an excellent fit to the experimental dispersions as shown by Regnault *et al.* in reference [22] with parameters obtained there as $\Delta_a^+ = 10.65$ meV, $\Delta_a^- = 8.75$ meV, $\delta^+ = 0.4$ meV, $\delta^- = 0.5$ meV. Note that this dispersion proposed by Regnault *et al.* [22] and derived in the present model has only *half* the period in q_x as compared to the pure zig-zag model of Figure 1b and equation (21). Using the empirical parameters from above and equation (39) one may completely determine the relevant parameters in the present theoretical model: $J_d^z = 38$ meV, $J_l = 0.11$ meV for intra- and inter-chain exchange respectively and for the intra-chain anisotropies we have $J_z - J_x = 1.49$ meV and $J_z - J_y = 1$ meV. Note that our model result for $\delta^\pm$ below equation (39) requires $\delta^+/\delta^- = \Delta^+/\Delta^-$. Experimentally $\delta^+/\delta^- = 0.80$ and $\Delta^+/\Delta^- = 0.82$ which is close to expectation. The dispersion obtained from equation (37) (or approximately from Eq. (39)) with these parameters is shown in Figure 7. Finally we comment on the question of intensities. Since we have two chemical sublattices separated by $\mathbf{d} = \frac{2}{3}\mathbf{a} + \mathbf{b}$ (Fig. 6b). and only sublattices of opposite spins are coupled in pairs the intensities will be given by a similar expression as in equation (23):

$$I_{\mathrm{A}}(\boldsymbol{\tau}) \sim \frac{1}{2}\left(1 + \cos\left(\frac{2\pi}{3}h\right)\right) = \cos^2\left(\frac{\pi}{3}h\right)$$
$$I_{\mathrm{O}}(\boldsymbol{\tau}) \sim \frac{1}{2}\left(1 - \cos\left(\frac{2\pi}{3}h\right)\right) = \sin^2\left(\frac{\pi}{3}h\right). \qquad (40)$$

In this case then the period of the intensity variation is correctly given by $h = 3$ as observed experimentally contrary to the zig-zag model of Figure 1b.

Sofar the dimerisation δ along **a** leading to $J_d \to (1 \pm \delta)J_d$ has been neglected. If included it would lead to an opening of an additional gap at the points $q_x = \pm\frac{\pi}{2}$ of size $2\delta\Delta_a$ as shown in Figure 7. Sofar this dimerization gap has not been identified. It is not clear whether the resolution is still too small or whether the inter-chain exchange dimerization $J_d(1 \pm \delta)$ of next neighbor zig-zag chains as shown in Figure 6b is indeed negligible. Another possibility is that a similar (symmetric) CO/MV structure as mentioned in the caption of Figure 6b is realized

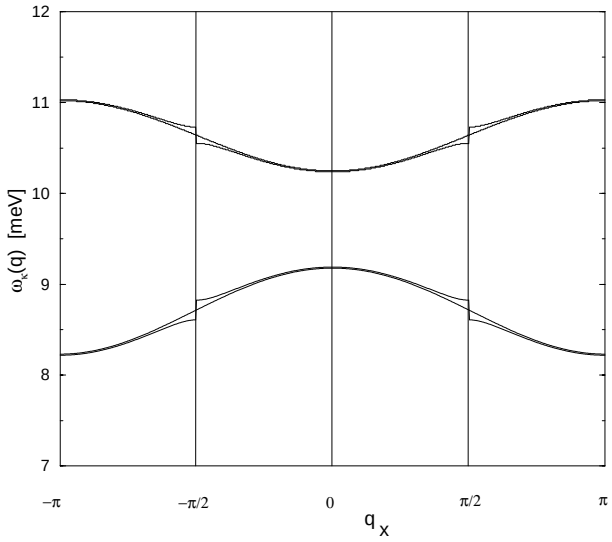

Fig. 7. Spin wave dispersion $\omega_\kappa(\mathbf{q})$ along q_x for $q_y = 0, \pi$ unfolded in the large BZ corresponding to the undistorted structure. Gapless curves: modes for zero dimerisation according to equation (37), gapped curves: modes with *perpendicular* dimerization according to Figure 6b with $\delta = 0.01$. This leads to small gaps at the boundary $(\pm\frac{\pi}{2})$ of the small BZ corresponding to the distorted structure. Exchange parameters and anisotropies have been chosen to comply with the experimentally determined dispersion by Regnault *et al.* [22] and given in the text of Section 4.5.

for which $\delta = 0$. In this structure, in the last terms of equations (36, 37) $\cos_y$ has to be replaced by one but the experimentally relevant equation (39) is unchanged.

5 Summary and conclusion

We have proposed and analyzed a number of spin-excitation models that may be relevant for inelastic neutron scattering investigations in the CO low temperature phase of $\alpha'-NaV_2O_5$. The most frequently discussed models are based on in-line or zig-zag chain CO and assume that the exchange coupling along the chains is much smaller than between the chains. In these models there is a strong dispersion along the chain axis $\mathbf{b}^*$ caused by the exchange coupling along the legs (in-line J) or ladder diagonals (zig-zag J_d). Recent LDA + U calculations [14] suggested that both are of the same order of magnitude. Therefore even in the completely CO zig-zag structure there is a strong dispersion $\parallel \mathbf{b}^*(q_y)$. The minimum excitation energy, *i.e.* the spin gap Δ_s in this scenario is due to a dimerization $J(1 \pm \delta)$ or $J_d(1 \pm \delta)$ of the intra-chain exchange. The dispersion $\parallel \mathbf{b}^*(q_x)$ on the other hand is comparatively small. However it shows characteristic differences for the two quasi-1D models. Allowing for small anisotropies in the largest exchange J or J_d we find that (1) the in-line model has a q_x-dispersionless splitting of the spin gap mode for $q_y = 0, \pi$ determined by the exchange anisotropy alone. The inter-chain coupling may only contribute to the q_x-dispersion at the maximum mode energy at $q_y = \frac{\pi}{2}$. This is a direct consequence of the Trellis lattice structure with every second ladder shifted by $\frac{b}{2}$. (2) in the zig-zag model the splitting of the $q_y = 0, \pi$ spin gap modes has both a contribution from exchange anisotropy $J_d^x - J_d^y$ and inter-chain coupling J'. Depending whether the former or latter is stronger one has little or noticeable dispersion along q_x and the role of anisotropy splitting and A-O splitting are interchanged. It was also shown that the magnetic field behaviour in the two limiting cases of the zig-zag model (Fig. 4) is different. While for J' appreciably larger than $J_x - J_y$ there is an almost linear Zeeman splitting of spin gap modes, they are almost field independent for small fields in the opposite case. In addition we discussed the zig-zag CO model in the case of strong coupling between the zig-zag chains because LDA + U calculations predict a surprisingly large inter-chain coupling J' in this CO-structure. In this case we used a broken symmetry approach to calculate the spin excitations. In this model the spin gap is a pure anisotropy gap, furthermore one obtains a split-off optical branch at an energy of 30 meV. The observation of such a mode would be crucial for this model, sofar there is no experimental evidence that it exists.

Furthermore we briefly discussed the alternative spin ladder model of Figure 6a with AF coupling in the ladder rungs. It was found that the dispersion along q_y has twice the periodicity as compared to the in-line and zig-zag chain models.

Perhaps the most promising model investigated is the mixed CO/MV model with zig-zag chains separated by disordered (MV) ladders. This structure model has been proposed in reference [23] and we have shown that it leads to spin wave dispersions exactly as those empirically proposed by Regnault *et al.* [22] from new inelastic neutrons scattering results. Most importantly it shows half the period for the dispersion along q_x as compared to the other models and also has the proper intensity variation. In this model the spin gap is due to a predominately Ising type exchange anisotropy and the dimerization perpendicular to the chains has only little effect.

All models discussed account for the basic qualitative properties of the available neutron scattering results [11]: (1) slightly split spin gap modes at $\Delta_s = 10$ meV with little or no dispersion along q_x and (2) a large dispersion of magnetic excitations along the chain (q_y)-direction. What is different in the models is the interpretation of the origin of various gaps and splittings observed, *i.e.* whether they are due to dimerization, anisotropy, ladder type or of A-O nature. To make further progress in discriminating between these models (and possibly others not investigated here) and also to obtain a more reliable set of exchange parameters for them it is necessary to have inelastic neutron scattering results in a larger energy and momentum region and with enhanced resolution and also a more detailed information on the momentum dependence of the intensity for each individual mode. The investigation in this paper has given a clear classification of the typical signatures of the different exchange models one has to look for.

P.T. would like to thank T. Yosihama for information on reference [18] and L.P. Regnault and T. Chatterji for helpful discussions.

References

1. M. Hase, I. Terasaki, K. Uchinokura, Phys. Rev. Lett. **70**, 3652 (1993).
2. M. Isobe, Y. Ueda, J. Phys. Soc. Jpn **65**, 1178 (1996).
3. H.G. v.Schnering, Yu. Grin, M. Knaupp, M. Somer, R.K. Kremer, O. Jepsen, T. Chatterji, M. Weiden, Z. Kristallogr. **213**, 246 (1998).
4. T. Chatterji, K.D. Liss, G.J. McIntyre, M. Weiden, C. Geibel, Sol. State Commun. **108**, 23 (1998).
5. H. Smolinski, C. Gros, W. Weber, U. Peuchert, G. Roth, M. Weiden, C. Geibel, Phys. Rev. Lett. **80**, 5164 (1998).
6. P. Fulde, Ann. Physik **6**, 178 (1997).
7. V.N. Antonov, A.N. Yaresko, A.Ya. Perlov, P. Thalmeier, P. Fulde, P.M. Oppeneer, H. Eschrig, Phys. Rev. B **58**, 9752 (1998).
8. P. Thalmeier, P. Fulde, Europhys. Lett. **44**, 242 (1998).
9. M. Köppen, D. Pankert, R. Hauptmann, M. Lang, M. Weiden, C. Geibel, F. Steglich, Phys. Rev. B **57**, 8466 (1998).
10. H. Seo, H. Fukuyama, J. Phys. Soc. Jpn **67**, 2602 (1998).
11. T. Yosihama, M. Nishi, K. Nakajima, K. Kakurai, Y. Fuji, M. Isobe, C. Kagami, Y. Ueda, J. Phys. Soc. Jpn **67**, 744 (1998).
12. T. Ohama, H. Yasuoka, M. Isobe, Y. Ueda, Phys. Rev. B **59**, 3299 (1999).
13. C. Gros, R. Valenti', Phys. Rev. Lett. **82**, 976 (1999).
14. A.N. Yaresko *et al.* (to be published).
15. G.S. Uhrig, H.J. Schulz, Phys. Rev. B **54**, R9624 (1996).
16. M. Azzouz, L. Chen, S. Moukouri, Phys. Rev. B **50**, 6233 (1994).
17. S. Gopalan, T.M. Rice, M. Sigrist, Phys. Rev. B **49**, 8901 (1994).
18. B. Leuenberger, A. Stebler, H.U. Güdel, A. Furrer, R. Feile, J.K. Kjems, Phys. Rev. B **30**, 6300 (1984).
19. J. des Cloizeaux, J.J. Pearson, Phys. Rev. **128**, 2131 (1962).
20. J. Jensen, A.R. Mackintosh, *Rare Earth Magnetism, Structures and Excitations* (Clarendon Press, Oxford, 1991).
21. J. Lüdecke, A. Jobst, S. van Smaalen, E. Morré, C. Geibel, H.-G. Krane, Phys. Rev. Lett. **82**, 3633 (1999).
22. L.-P. Regnault, J.E. Lorenzo, J.-P. Boucher, B. Grenier, A. Hiess, T. Chatterji, J. Jedougez, A. Revcolevschi (preprint).
23. S. van Smaalen, J. Lüdecke, Europhys. Lett. **49**, 250 (2000).
24. M. Oshikawa, I. Affleck, Phys. Rev. Lett. **79**, 2883 (1997).